Journal of Geography and Cartography 2025, 8(2), 11427.
https://doi.org/10.24294/jgc11427

Article

Modeling soil electrical conductivity using machine learning: Implications for sustainable land use in saline coastal regions

Ramin Samieifard[1,*], Patrick Joseph Drohan[1], Ahmad Heidari[2]

[1] Department of Ecosystem Science & Management, Pennsylvania State University, PA 16802, USA
[2] Soil Science Department, University of Tehran, Karaj 31587-77871, Iran
*** Corresponding author:** Ramin Samieifard, rks5845@psu.edu

CITATION

Samieifard R, Drohan PJ, Heidari A. Modeling soil electrical conductivity using machine learning: Implications for sustainable land use in saline coastal regions. Journal of Geography and Cartography. 2025; 8(2): 11427. https://doi.org/10.24294/jgc11427

ARTICLE INFO

Received: 27 January 2025
Accepted: 21 March 2025
Available online: 9 April 2025

Abstract: Soil salinization is a difficult challenge for agricultural productivity and environmental sustainability, particularly in arid and semi-arid coastal regions. This study investigates the spatial variability of soil electrical conductivity (EC) and its relationship with key cations and anions (Na^+, K^+, Ca^{2+}, Mg^{2+}, Cl^-, CO_3^{2-}, HCO_3^-, SO_4^{2-}) along the southeastern coast of the Caspian Sea in Iran. Using a combination of field-based soil sampling, laboratory analyses, and Landsat 8 spectral data, linear Multiple Linear Regression and Partial Least Squares Regression (MLR, PLSR) and nonlinear Artifician Neural Network and Support Vector Machine (ANN, SVM) modeling approaches were employed to estimate and map soil EC. Results identified Na^+ and Cl^- as the primary contributors to salinity (r = 0.78 and r = 0.88, respectively), with NaCl salts dominating the region's soil salinity dynamics. Secondary contributions from Potassium Chloride KCl and Magnesium Chloride $MgCl_2$ were also observed. Coastal landforms such as lagoon relicts and coastal plains exhibited the highest salinity levels, attributed to geomorphic processes and anthropogenic activities. Among the predictive models, the SVM algorithm outperformed others, achieving higher R^2 values and lower RMSE ($RMSE_{Test}$ = 27.35 and $RMSE_{Train}$ = 24.62, respectively), underscoring its effectiveness in capturing complex soil-environment interactions. This study highlights the utility of digital soil mapping (DSM) for assessing soil salinity and provides actionable insights for sustainable land management, particularly in mitigating salinity and enhancing agricultural practices in vulnerable coastal systems.

Keywords: electrical conductivity; SVM; salinity; coastal landforms; remote sensing

1. Introduction

Soil electrical conductivity (EC) is widely recognized as a reliable indicator for assessing soil salinity and monitoring soil salinization. EC values directly correlate with the ionic concentration of the soil solution, increasing as salt content rises under specific moisture conditions [1]. However, a major challenge in soil quality assessment lies in addressing the significant spatial and temporal variability of soil properties across different observational scales [2].

Soil salinization and sodification represent critical processes of soil degradation, posing significant threats to ecosystems, particularly in arid and semi-arid regions. These processes profoundly affect agricultural productivity and sustainability by altering soil properties and reducing fertility. Sodium (Na^+) dominance in the soil solution leads to the dispersion of clay particles, which disrupts soil structure and significantly decreases soil permeability. Among the salts contributing to salinization, their impact decreases in the order of NaCl > $CaSO_4^{2-}$ > $CaHCO_3$ > $MgCl_2$ > $Mg(HCO_3)_2$. Elevated salinity negatively influences all aspects of plant growth by

disrupting ion uptake balance, inducing osmotic stress, and impairing water absorption by plant roots [3–5].

According to the U.S. Salinity Laboratory standards, soils are classified as saline when their electrical conductivity of the saturation extract (ECe) exceeds 4 $dS \cdot m^{-1}$ at 25 °C, with an Exchangeable Sodium Percentage (ESP) below 15 and a pH less than 8.5. These soils are characterized by high concentrations of ions such as Na^+, Mg^{2+}, Ca^{2+}, sulfate (SO_4^{2-}), and chloride (Cl^-) [6]. Ion detection in soils is critical across various domains, including human health, food security, and environmental monitoring, as ion concentrations provide vital information about soil and water quality. For instance, the analysis of ions such as calcium (Ca^{2+}), sodium (Na^+), potassium (K^+), and magnesium (Mg^{2+}) is essential in evaluating water suitability for human consumption and agricultural irrigation. Elevated concentrations of these ions are indicative of increased soil salinity or sodicity, which can adversely affect plant growth. Similarly, ion monitoring plays a crucial role in food processing, with specific ions such as nitrate (NO_3^-) and nitrite (NO_2^-) in meat products, calcium (Ca^{2+}) in dairy, and potassium (K^+) in fruit juices being key indicators of food safety and quality [7,8].

Coastal regions, where terrestrial and marine ecosystems converge, are highly susceptible to soil salinization driven by both natural processes and anthropogenic activities. These areas support a significant proportion of the global population and are characterized by high biodiversity and unique ecological features. Additionally, coastal zones function as hubs for economic, agricultural, and recreational activities. However, rapid population growth and escalating freshwater demands have intensified the intrusion of seawater into groundwater reserves. This saltwater intrusion elevates groundwater salinity, which subsequently migrates into the rhizosphere through capillary action, depositing salt minerals. This process adversely affects soil fertility, reducing crop yields and, in severe cases, causing complete crop failure [6,9].

Remote sensing is an essential tool for multi-scale and long-term monitoring of soil salinization due to its efficiency in acquiring extensive datasets over large areas. However, factors such as atmospheric conditions, soil-atmosphere electromagnetic radiation interactions, and overlapping spectral signals from different soil components can significantly reduce the accuracy of remotely sensed data, often resulting in inconsistent outcomes. Consequently, remote sensing is predominantly employed for mapping the spatial distribution of soil salinity and classifying salinity levels, rather than generating precise quantitative measurements [10–12].

To improve the reliability of remote sensing applications, researchers frequently integrate satellite imagery and remotely sensed data with ground-based field and laboratory measurements to estimate and map soil properties [13,14]. Linear multivariate models, such as Multiple Linear Regression (MLR) and Partial Least Squares Regression (PLSR), have been successfully applied to analyze spectral absorption patterns and their relationships with soil characteristics. In recent years, nonlinear modeling approaches, including Support Vector Machines (SVM) and Artificial Neural Networks (ANN), have gained prominence for their superior ability to capture complex interactions between soil physical and chemical properties and spectral data [15,16].

The primary objectives of this research were to:

(1) Assess the relationship between soil electrical conductivity and ion

concentrations: Investigate the correlation between soil electrical conductivity (ECe) and the concentrations of key cations (Na^+, K^+, Ca^{2+}, Mg^{2+}) and anions (Cl^-, CO_3^{2-}, HCO_3^-, SO_4^{2-}) to identify the dominant drivers of soil salinity that could negatively affect agriculture.

(2) Characterize spatial variability of soil salinity: Map and analyze the spatial distribution of soil salinity and its association with geomorphological landforms, including lagoons, lagoon relicts, coastal plains, and barriers, to understand the influence of geomorphic processes on salinity dynamics.

(3) Evaluate the performance of Digital Soil Mapping (DSM) algorithms for salinity landscape modeling: Compare the predictive accuracy of linear models (Multiple Linear Regression [MLR] and Partial Least Squares Regression [PLSR]) and nonlinear models (Support Vector Machines [SVM] and Artificial Neural Networks [ANN]) in estimating soil EC and ion distributions using Landsat 8 spectral data.

(4) Develop a framework for soil salinity monitoring and management to support agriculture: Provide actionable insights for land management by integrating DSM outputs with geomorphological analysis to inform sustainable agricultural practices and salinity mitigation strategies in vulnerable coastal regions.

These objectives aim to advance the understanding of soil salinity dynamics while leveraging modern remote sensing and modeling approaches to support sustainable land use and agricultural productivity in semi-arid climates with salinity management concerns.

2. Methods

2.1. Study area

The study was conducted over a 480 km^2 area along the southeastern coast of the Caspian Sea in Iran, spanning from 54°21′10″ E, 37°18′57″ N to 53°54′58″ E, 37°18′57″ N (**Figure 1**). This region has a semi-arid climate, with an average annual temperature of 17.6 ℃ and annual precipitation of 350 mm [17,18]. The landscape comprises diverse coastal landforms, including lagoons, lagoon relicts, coastal plains, and barriers, each significantly influencing soil salinity dynamics. These landforms are particularly susceptible to salinization due to geomorphic processes and agricultural activities, making them an ideal setting for investigating the spatial variability of soil electrical conductivity (EC) [19,20].

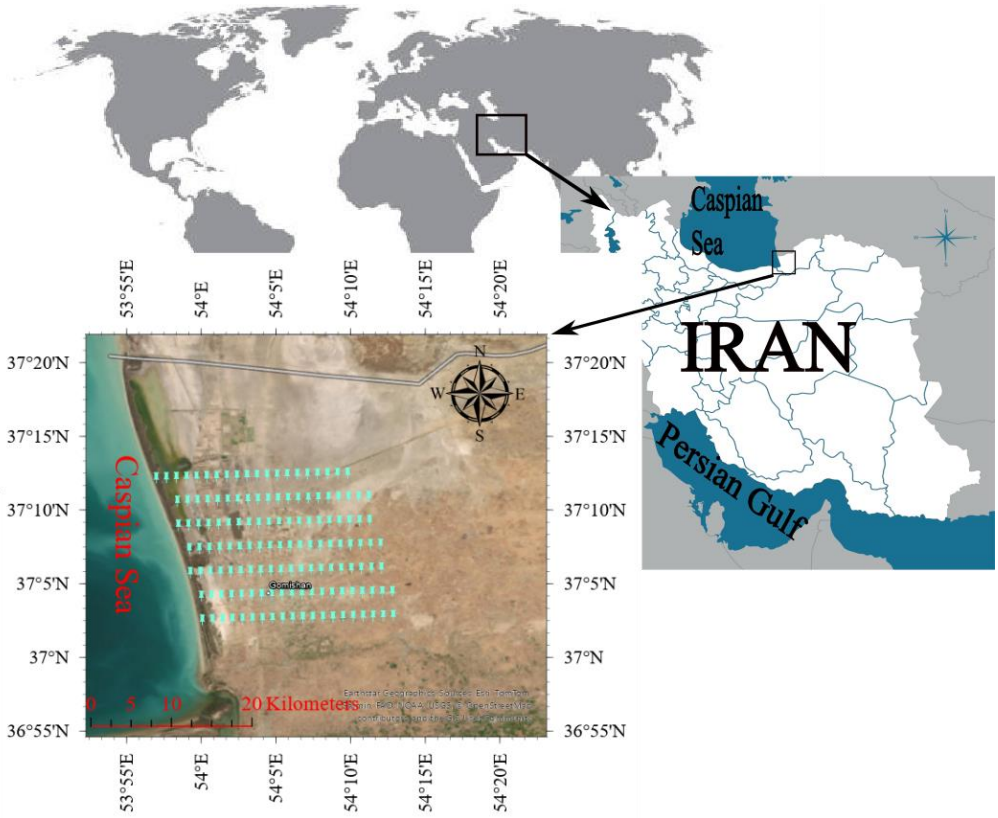

Figure 1. Setting of the study area.

2.2. Sampling

A systematic grid-based sampling network was established, comprising seven parallel rows spaced 3 km apart, with 20 sampling points per row at 1 km intervals. Soil samples were collected from the top 20 cm of the soil profile. The samples were air-dried, sieved through a 2-mm mesh, and subjected to laboratory analysis. The electrical conductivity (EC) of the soil-saturated extracts was measured using an EC meter.

Cation (Na^+, K^+, Ca^{2+}, Mg^{2+}) and anion (Cl^-, CO_3^{2-}, HCO_3^-, SO_4^{2-}) concentrations were analyzed following the standardized protocols outlined in the methods of soil analysis [21]. These methods ensured precise quantification of ion concentrations, facilitating robust correlation analyses between ion content and soil EC. The resulting dataset provided a reliable foundation for calibrating remote sensing models and enhancing the understanding of salinity dynamics within the study area.

This study employed statistical analyses, including Multiple Linear Regression (MLR), Partial Least Squares Regression (PLSR), Artificial Neural Networks (ANN), and Support Vector Machines (SVM), to estimate and map soil electrical conductivity (EC). The Digital Elevation Model (DEM) data was obtained from the Iranian Mapping Organization [19,20]. The primary software used for data processing and modeling included GIS tools for spatial analysis and machine learning platforms (MATLAB 2019b) for predictive modeling. The predictive models incorporated key soil variables such as Na^+, K^+, Ca^{2+}, Mg^{2+}, Cl^-, CO_3^{2-}, HCO_3^-, and SO_4^{2-}, sourced from laboratory analyses and spectral data from Landsat 8 imagery. In particular, the SVM model used a Gaussian kernel, which contributed to its superior predictive

performance. The methodology involved field soil sampling, laboratory analysis, spectral data extraction, and statistical modeling to establish relationships between soil properties and salinity dynamics, providing a comprehensive framework for soil salinity assessment in coastal environments.

3. Results

Principal Component Analysis (PCA) was employed to evaluate the relationships between soil electrical conductivity (ECe) and the concentrations of laboratory-measured cations and anions (Na^+, K^+, Ca^{2+}, Mg^{2+}, Cl^-, CO_3^{2-}, HCO_3^-, and SO_4^{2-}). As illustrated in **Figure 2a**, Cl^- exhibited the strongest correlation with ECe (r = 0.88), followed by Na^+ (r = 0.78), indicating their dominant influence on soil salinity in the study area. Soil K^+, Mg^{2+}, and SO_4^{2-} were the next most influential ions, with correlation values of 0.69, 0.69, and 0.51, respectively. Among the cations, Ca^{2+} demonstrated the lowest impact on ECe (r = 0.30), while CO_3^{2-} and HCO_3^- had negligible or negative correlations (r = 0.02 and −0.28, respectively).

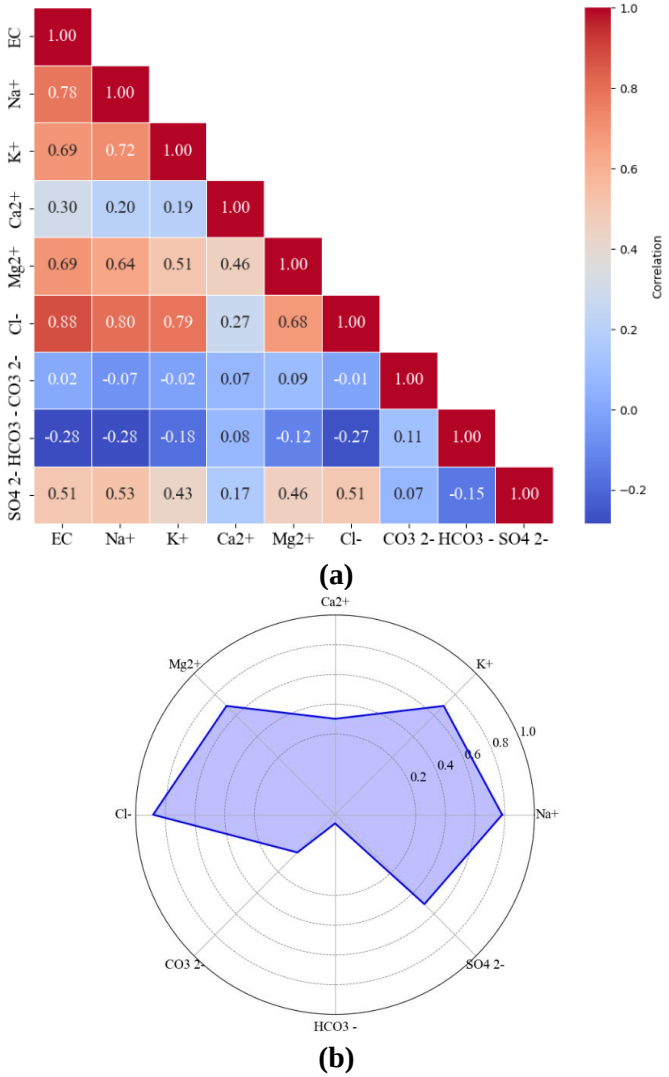

Figure 2. (a) Correlation heatmap of EC with cations and anions; **(b)** radar chart of the effect of each ion on the EC.

Figure 2b provides a visual representation of the relationships between the investigated ions and EC, highlighting the relative influence of each ion on soil ECe. These findings confirm that NaCl salts are the primary drivers of soil salinity in the southeastern Caspian Sea region. Further analysis of the correlation heatmap reveals that KCl salts have a comparable effect on ECe, as evidenced by the strong correlations among Na^+, K^+, and Cl^-. Additionally, the significant relationship between Mg^{2+} and Cl^- ($r = 0.68$) underscores the greater impact of Mg^{2+} on ECe compared to Ca^{2+}. These results emphasize the importance of specific ions in shaping the salinity dynamics of the study area.

Figure 3 illustrates the distribution patterns of the analyzed cations (Na^+, K^+, Ca^{2+}, Mg^{2+}) and anions (Cl^-, CO_3^{2-}, HCO_3^-, SO_4^{2-}) as predicted by the Support Vector Machine (SVM) algorithm. **Figure 4** depicts the detected coastal landforms in the study area, mapped by the authors using the Geopedological Definition System (GDS) and Zinck's geopedology approach, integrating particle size distribution (PSD) analysis and digital elevation model (DEM) data [19,20].

Figure 3 maps reveal that the lowest to moderate values of Na^+, K^+, Ca^{2+}, Mg^{2+}, Cl^-, CO_3^{2-}, HCO_3^-, SO_4^{2-}, and soil EC are predominantly associated with the modern lagoon landform in the western part of the study area, located between the present-day barrier (near the current shoreline) and the old barrier (east of the modern lagoon). Conversely, the highest EC values are concentrated in the coastal plain and lagoon relict landforms, situated in the central and southeastern portions of the study area.

A strong alignment exists between the EC distribution and the patterns of Na^+ and Cl^- (**Figure 3**: Na^+ and Cl^-), followed by K^+, Mg^{2+}, and SO_4^{2-} (**Figure 3**: K^+, Mg^{2+}, and SO_4^{2-}); these results are consistent with the validation metrics presented in **Table 1**, which detail the correlation coefficients, relative percent differences (RPD), and root mean square errors (RMSE) obtained using both linear (MLR, PLSR) and nonlinear (ANN, SVM) algorithms. The superior performance of SVM and ANN models in capturing the complex relationships between soil EC and ion content further validates these observations.

Our results show that the Support Vector Machine (SVM) algorithm provided more accurate predictions of soil electrical conductivity (EC). In this regard, the SVM provided better predictions for associated cations and anions using Landsat 8 spectral data compared to Artificial Neural Networks (ANN), Multiple Linear Regression (MLR), and Partial Least Squares Regression (PLSR) models (**Table 1**). The average soil EC across sampled points was approximately 45 $dS \cdot m^{-1}$, consistent with the spatial distribution patterns observed in the generated maps, particularly in regions represented by green and blue color codes (refer to the map legend).

Our validation results suggest the SVM and ANN models provide superior performance, with Relative Percent Difference (RPD) values exceeding 1.1, indicating good model reliability. In contrast, the MLR and PLSR models, which had RPD values below 1.1, were less effective in estimating soil EC from Landsat 8 data [22]. Root Mean Square Error (RMSE) values also indicated lower prediction errors for SVM and ANN compared to the linear models, MLR and PLSR. Additionally, the coefficient of determination (R^2) values for the nonlinear models (SVM and ANN) were significantly higher than those of the linear models, reinforcing the enhanced predictive capability of nonlinear approaches in capturing the complex relationships

between soil properties and spectral data.

Table 1. Validation results in estimations and mapping of soil EC using different models.

		RMSE test	**RMSE train**	**RPD test**	**RPD train**	***R*² test**	***R*² train**
SVM	EC	27.35	24.62	1.18	1.29	0.36	0.46
	Na	236.83	283.97	1.19	1.11	0.45	0.29
	K	2.28	3.27	1.48	1.31	0.64	0.48
	Ca	16.71	14.01	1.97	1.13	0.26	0.30
	Mg	195.50	164.68	1.05	1.13	0.17	0.37
	Cl	195.50	164.68	1.05	1.13	0.25	0.44
	CO_3^{2-}	0.26	0.29	1.44	1.35	0.69	0.52
	HCO_3^-	0.60	0.86	1.26	1.14	0.42	0.36
	SO_4^{2-}	42.27	38.82	1.14	1.15	0.40	0.31
ANN	EC	27.69	25.85	1.17	1.23	0.27	0.34
	Na	237.14	257.17	1.19	1.22	0.29	0.34
	K	2.43	2.99	1.39	1.20	0.51	0.32
	Ca	25.96	13.60	1.20	1.16	0.36	0.26
	Mg	193.48	155.53	1.06	1.20	0.12	0.31
	Cl	361.58	217.52	1.11	1.44	0.22	0.52
	CO_3^{2-}	0.35	0.35	1.06	1.19	0.12	0.15
	HCO_3^-	0.58	0.82	1.30	1.20	0.43	0.31
	SO_4^{2-}	42.30	41.44	1.14	1.07	0.28	0.14
MLR	EC	30.70	30.82	1.06	1.03	0.11	0.06
	Na	269.84	301.14	1.04	1.04	0.08	0.08
	K	3.13	3.60	1.08	1.00	0.15	0.01
	Ca	26.04	15.70	0.99	1.00	0.02	0.02
	Mg	203.42	180.68	1.01	1.03	0.03	0.06
	Cl	203.42	180.68	1.01	1.03	0.01	0.13
	CO_3^{2-}	0.37	0.32	1.02	1.00	0.14	0.12
	HCO_3^-	0.70	0.97	1.07	1.02	0.23	0.04
	SO_4^{2-}	46.08	43.47	1.04	1.02	0.10	0.05
PLSR	EC	30.95	30.96	1.05	1.02	0.10	0.05
	Na	278.97	307.53	1.01	1.02	0.03	0.05
	K	3.13	3.60	1.08	1.00	0.15	0.01
	Ca	26.04	15.70	0.99	1.00	0.02	0.02
	Mg	203.42	180.68	1.01	1.03	0.03	0.06
	Cl	414.95	297.49	0.97	1.05	0.07	0.11
	CO_3^{2-}	0.37	0.329	1.01	1.00	0.11	0.01
	HCO_3^-	0.75	0.99	1.00	1.00	0.06	0.01
	SO_4^{2-}	46.08	43.47	1.04	1.023	0.097	0.05

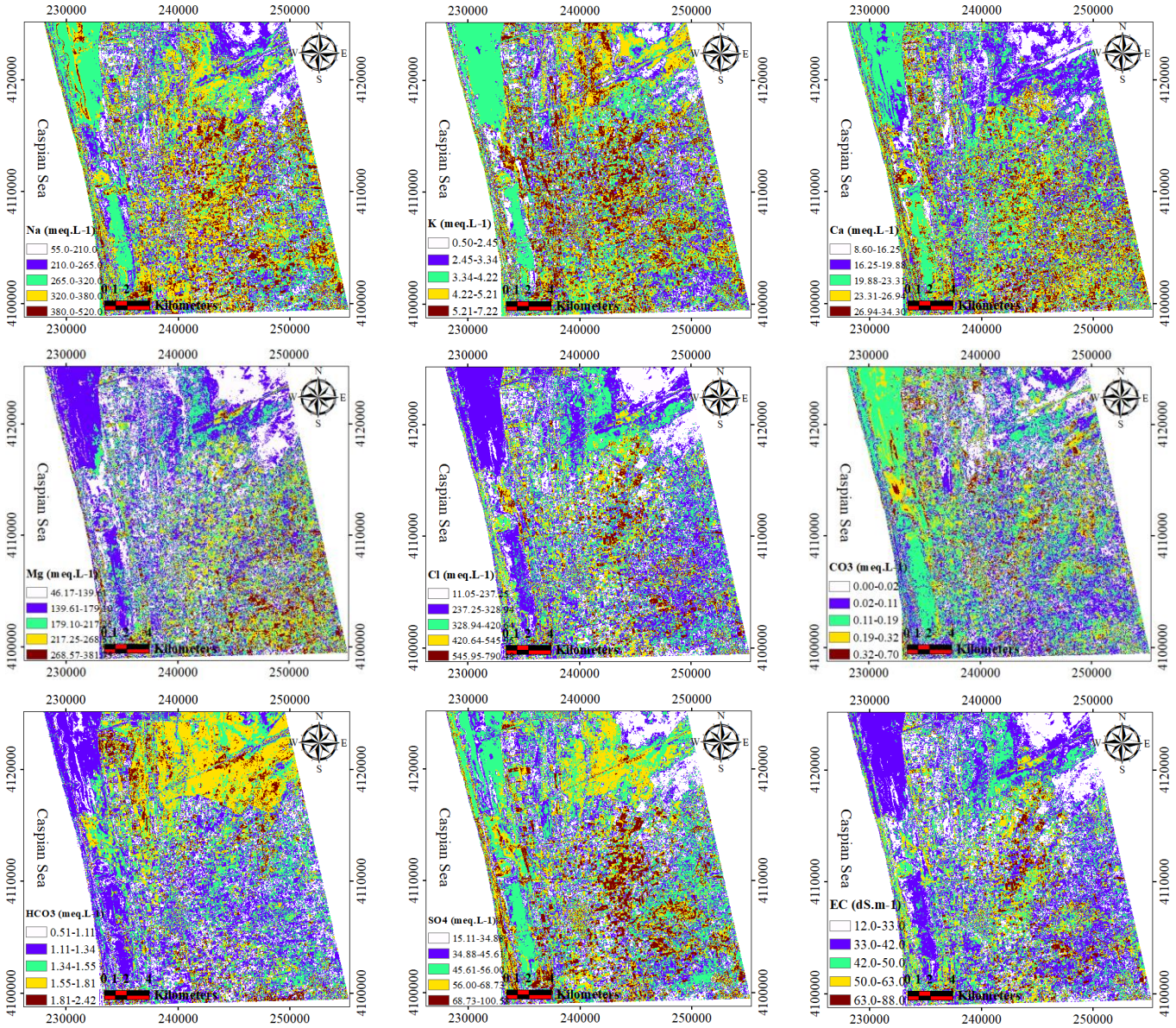

Figure 3. Distribution maps of Na^+, K^+, Ca^{2+}, Mg^{2+}, Cl^-, CO_3^{2-}, HCO^{3-}, and SO_4^{2-} (m eq·L^{-1}), soil EC (dS·m^{-1}) in the study area.

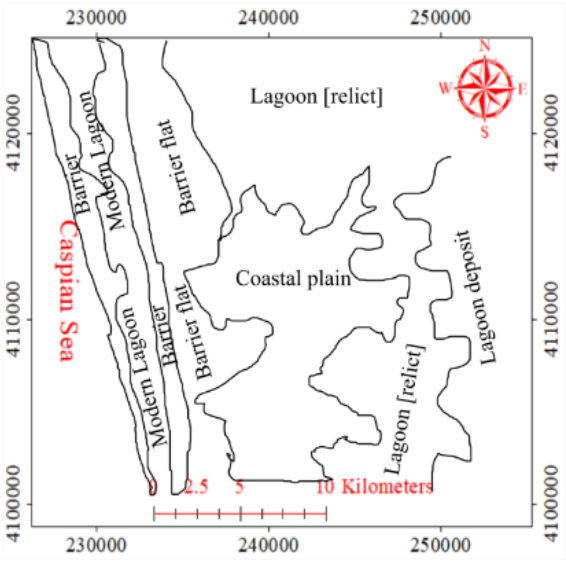

Figure 4. Detected landforms based on GDS and soil EC distribution maps of the study area.

4. Discussion

The efficiency of digital soil mapping (DSM) in generating categorical soil property maps is influenced by several factors, including cost-effectiveness, sampling resolution, model accuracy, and the chosen scale of mapping [14]. The study area along the southeastern coast of the Caspian Sea exhibits high salinity levels, classifying it as a very saline region. Agricultural activities in this area depend heavily on effective soil drainage and reclamation measures, alongside the cultivation of salt-tolerant crops such as barley. Field observations confirmed that rainfed barley is the dominant crop, aligning with the traditional practices of local communities, including the Turkmen Sahara's reliance on camel and horse breeding for livelihoods.

4.1. Impact of soil EC on coastal landforms

Land degradation driven by soil salinity, flooding, and overuse of fields is a significant factor reducing soil productivity in the region [23]. This study emphasizes the influence of coastal landforms on soil electrical conductivity (EC) patterns and productivity. Six distinct landforms were identified using the Geopedological Definition System (GDS) and Zinck's geopedology approach [24], including lagoons, lagoonal deposits, barriers, and coastal plains. These landforms exhibit a clear relationship between geomorphological processes and soil EC.

Lagoonal landforms, defined as shallow saline or brackish water bodies separated from the sea by barriers, were found to contain soils with elevated salinity. This observation aligns with the study's results, which showed high EC values in these areas. Barriers and barrier flats, described as subaerial and gently sloping landforms adjacent to lagoons, exhibited increased EC levels at their edges, with a sharp decline within the barrier flats, likely due to sediment movement and leaching processes. These findings suggest that the dynamic interplay of geomorphic processes and saline water transport significantly influences EC distribution.

The highest EC levels were observed in coastal plains and lagoon relict

landforms, which represent remnants of old lagoons. These features remain largely unburied, preserving the saline characteristics of their historical environments. The similarity in EC distribution patterns between lagoonal deposits and these landforms underscores the critical role of past hydrological and geomorphological conditions. Lagoonal deposits, primarily composed of sand, silt, or clay transported by wind, flux flows, and currents, were deposited in low-energy saline environments. The observed alignment of EC patterns in these sediments with those in coastal plains and lagoon relics reinforces the connection between landform genesis and soil salinity (**Figure 2**).

4.2. Contributions of cations, anions, and PCA analysis

Principal Component Analysis (PCA) revealed Cl^- and Na^+ as the primary contributors to soil EC, exhibiting the strongest correlations. These findings highlight the dominant role of NaCl salts in driving salinity in the region. Moderate correlations between K^+, Mg^{2+}, and SO_4^{2-} with EC suggest the additional influence of salts such as KCl. The strong relationship between Mg^{2+} and Cl^- further indicates the significant impact of Mg^{2+} on soil salinity, surpassing that of Ca^{2+}, which showed the lowest correlation among the investigated cations. The negligible or negative correlations of CO_3^{2-} and HCO_3^- with EC confirm their limited role in salinity dynamics in this area, consistent with the dominance of chloride-based salts.

4.3. Performance of DSM algorithms

The study validated the performance of DSM algorithms in mapping soil salinity and related properties using Landsat 8 spectral data. Among the models evaluated, the Support Vector Machine (SVM) algorithm demonstrated superior accuracy in predicting soil EC and cation/anion concentrations, outperforming ANN, MLR, and PLSR models. This was evident from higher R^2 and RPD values and lower RMSE scores for SVM and ANN compared to the poorer performance of MLR and PLSR. These findings align with prior research [22] emphasizing the advantages of non-linear models in capturing complex soil-environment interactions. The SVM algorithm's ability to accurately predict EC and ion distribution patterns underscores its effectiveness for soil mapping in saline environments.

4.4. Implications for land management

The observed spatial patterns in soil EC and ion distributions underscore the need for targeted reclamation strategies across coastal landforms. High salinity levels in lagoonal deposits and coastal plains necessitate focused interventions, such as improved drainage and salinity mitigation measures. In contrast, barrier flats and modern lagoons, with relatively lower salinity, present opportunities for cultivating salt-tolerant crops like barley. By integrating geomorphological analysis with DSM outputs, this study provides actionable insights into the spatial variability of soil salinity. These findings can guide sustainable land management practices, promoting soil productivity and environmental conservation in vulnerable coastal agricultural systems.

4.5. Practical applications and perspectives

The findings of this study provide valuable insights into sustainable land management and soil salinity mitigation in coastal agricultural regions. By leveraging DSM techniques, policymakers and land managers can implement targeted interventions to enhance soil productivity. The high spatial variability of soil EC suggests the need for adaptive management strategies, including the promotion of salt-tolerant crops such as barley in high-salinity areas and the implementation of effective artificial drainage systems to reduce salt accumulation. Additionally, the identification of coastal landforms with distinct salinity patterns enables site-specific reclamation approaches, optimizing land use planning in vulnerable regions. From a broader perspective, this study highlights the importance of using remote sensing data, machine learning algorithms, and geomorphological analysis for environmental monitoring. The superior performance of SVM models underscores their potential for refining predictive soil mapping techniques, which could be further enhanced by incorporating additional high-resolution spectral datasets. Future research could explore the impact of climate variability on salinity dynamics, integrating temporal monitoring to develop long-term mitigation strategies. By expanding the application of DSM in other arid and semi-arid coastal areas, these methodologies can contribute to global efforts in combating soil degradation and ensuring agricultural sustainability.

5. Conclusion

This study underscores the importance of understanding soil salinity dynamics in coastal regions, particularly in the southeastern Caspian Sea, where salinization poses significant challenges to agricultural productivity and environmental sustainability. The research confirms that soil electrical conductivity (EC) is a reliable indicator of salinity, with chloride (Cl^-) and sodium (Na^+) emerging as the primary contributors. Secondary influences from potassium (K^+), magnesium (Mg^{2+}), and sulfate (SO_4^{2-}) further emphasize the complex interactions among soil ions in shaping salinity patterns.

The findings reveal distinct spatial variability in soil EC linked to geomorphological processes and landform characteristics. Lagoonal deposits, coastal plains, and lagoon relict landforms exhibit the highest salinity levels, reflecting their susceptibility to saline water intrusion and historical geomorphic conditions. Conversely, barrier flats and modern lagoons demonstrate lower salinity levels, offering potential for sustainable agricultural practices.

In terms of methodology, the study highlights the superiority of nonlinear modeling approaches, particularly the Support Vector Machine (SVM) algorithm, in predicting soil EC and ion distributions using Landsat 8 spectral data. SVM outperformed other models, including Artificial Neural Networks (ANN), Multiple Linear Regression (MLR), and Partial Least Squares Regression (PLSR), as evidenced by higher R^2 values, lower RMSE scores, and better Relative Percent Difference (RPD) values. These results validate the utility of nonlinear models for capturing complex soil-environment interactions in digital soil mapping (DSM).

The implications for land management are clear: effective salinity mitigation strategies must target high-risk areas, such as lagoonal deposits and coastal plains,

through improved drainage and soil reclamation measures. Meanwhile, the lower salinity in barrier flats and modern lagoons supports the cultivation of salt-tolerant crops, such as barley. By integrating geomorphological analysis with DSM outputs, this study provides a robust framework for addressing soil salinity challenges, enabling more informed and sustainable land use practices in coastal agricultural systems.

Limitations of the study

Despite its valuable contributions, the present study has certain limitations. The reliance on Landsat 8 spectral data, while effective, may not capture fine-scale variations in soil salinity as accurately as higher-resolution remote sensing technologies such as hyperspectral or UAV-based imagery. Additionally, the study's focus on a specific coastal region limits the generalizability of the findings to other environments with various climatic and geomorphological conditions. The use of DSM models, particularly SVM, though robust, may benefit from further optimization by incorporating additional environmental covariates such as groundwater depth and soil moisture dynamics. Future research should address the mentioned restrictions by integrating multi-source data and expanding frequent monitoring to assess long-term salinity trends under changing environmental conditions.

Author contributions: Conceptualization, RS and PJD; methodology, RS; software, RS; validation, RS, PJD and AH; formal analysis, RS; investigation, RS; resources, RS and AH; data curation, AH; writing—original draft preparation, RS; writing—review and editing, PJD; visualization, RS; supervision, AH and PJD; project administration, AH; funding acquisition, AH. All authors have read and agreed to the published version of the manuscript.

Institutional review board statement: Not applicable.

Informed consent statement: Not applicable.

Conflict of interest: The authors declare no conflict of interest.

References

1. Zhang Z, Ren J, Wang Y, et al. Study on the EC prediction of cracked soda saline-alkali soil based on texture analysis of high-resolution images from ground-based observation and machine learning methods. Soil and Tillage Research. 2024; 244: 106234. doi: 10.1016/j.still.2024.106234
2. Iseas MS, Sainato CM, Gómez A, et al. Assessing salinity and sodicity of irrigated soils using apparent electrical conductivity in the Pampean region. Environmental Earth Sciences. 2024; 83(12). doi: 10.1007/s12665-024-11643-w
3. Abdullahi M, Elnaggar A, Omar M, et al. Land degradation, causes, implications and sustainable management in arid and semi arid regions: a case study of Egypt. Egyptian Journal of Soil Science. 2023; 63(4): 0-0. doi: 10.21608/ejss.2023.230986.1647
4. Elmeknassi M, Elghali A, de Carvalho HWP, et al. A review of organic and inorganic amendments to treat saline-sodic soils: Emphasis on waste valorization for a circular economy approach. Science of The Total Environment. 2024; 921: 171087. doi: 10.1016/j.scitotenv.2024.171087
5. González-Nava VJ, Solís-Valdéz S, Manríquez J, et al. Detection of sodium ion in aqueous soil extract using Prussian blue modified screen-printed electrodes. Electrochimica Acta. 2025; 513: 145564. doi: 10.1016/j.electacta.2024.145564
6. Kumar P, Tiwari P, Biswas A, et al. Spatio-temporal assessment of soil salinization utilizing remote sensing derivatives, and prediction modeling: Implications for sustainable development. Geoscience Frontiers. 2024; 15(6): 101881. doi:

10.1016/j.gsf.2024.101881
7. González-Nava VJ, Cárdenas Mijangos J, Frausto-Castillo RF, et al. Hemodialysis Wastewater Treatment via Electrocoagulation and Electro-Oxidation: Modular Pilot-Level Modeling and Simulation. ChemPlusChem. 2024; 89(6). doi: 10.1002/cplu.202300671
8. Xing J, Li X, Li Z, et al. Remediation of soda-saline-alkali soil through soil amendments: Microbially mediated carbon and nitrogen cycles and remediation mechanisms. Science of The Total Environment. 2024; 924: 171641. doi: 10.1016/j.scitotenv.2024.171641
9. Sheng D, Meng X, Wen X, et al. Hydrochemical characteristics, quality and health risk assessment of nitrate enriched coastal groundwater in northern China. Journal of Cleaner Production. 2023; 403: 136872. doi: 10.1016/j.jclepro.2023.136872
10. Hill AC. Land-atmosphere carbon dioxide and methane exchange in a temperate salt marsh. University of Delaware; 2023.
11. Rafik A, Ibouh H, El Alaoui El Fels A, et al. Soil Salinity Detection and Mapping in an Environment under Water Stress between 1984 and 2018 (Case of the Largest Oasis in Africa-Morocco). Remote Sensing. 2022; 14(7): 1606. doi: 10.3390/rs14071606
12. Wang F, Han L, Liu L, et al. Advancements and Perspective in the Quantitative Assessment of Soil Salinity Utilizing Remote Sensing and Machine Learning Algorithms: A Review. Remote Sensing. 2024; 16(24): 4812. doi: 10.3390/rs16244812
13. Diaz-Gonzalez FA, Vuelvas J, Correa CA, et al. Machine learning and remote sensing techniques applied to estimate soil indicators – Review. Ecological Indicators. 2022; 135: 108517. doi: 10.1016/j.ecolind.2021.108517
14. Zeraatpisheh M, Ayoubi S, Jafari A, et al. Comparing the efficiency of digital and conventional soil mapping to predict soil types in a semi-arid region in Iran. Geomorphology. 2017; 285: 186-204. doi: 10.1016/j.geomorph.2017.02.015
15. Nouri A, Esfandiari M, Eftekhari K, et al. Development support vector machine, artificial neural network and artificial neural network – genetic algorithm hybrid models for estimating erodible fraction of soil to wind erosion. International Journal of River Basin Management. 2023; 22(3): 379-388. doi: 10.1080/15715124.2022.2153856
16. Alomar S, Mireei SA, Hemmat A, et al. Comparison of Vis/SWNIR and NIR spectrometers combined with different multivariate techniques for estimating soil fertility parameters of calcareous topsoil in an arid climate. Biosystems Engineering. 2021; 201: 50-66. doi: 10.1016/j.biosystemseng.2020.11.007
17. Kakroodi AA, Kroonenberg SB, Hoogendoorn RM, et al. Rapid Holocene sea-level changes along the Iranian Caspian coast. Quaternary International. 2012; 263: 93-103. doi: 10.1016/j.quaint.2011.12.021
18. Kakroodi AA, Kroonenberg SB, Beni AN, et al. Short- and Long-Term Development of the Miankaleh Spit, Southeast Caspian Sea, Iran. Journal of Coastal Research. 2014; 298: 1236-1242. doi: 10.2112/jcoastres-d-12-00174.1
19. Samiei-Fard R, Heidari A, Drohan PJ, et al. The Effect of Using a Geopedological Approach in Determining Land Quality Indicators, Land Degradation, and Development (Case Study: Caspian Sea Coast). Environments. 2024; 11(1): 20. doi: 10.3390/environments11010020
20. Samiei-Fard R, Heidari A, Konyushkova M, et al. Application of particle size distribution throughout the soil profile as a criterion for recognition of newly developed geoforms in the Southeastern Caspian coast. CATENA. 2021; 203: 105362. doi: 10.1016/j.catena.2021.105362
21. Sparks DL, Page AL, Helmke PA, Loeppert RH. Methods of soil analysis, part 3: Chemical methods. John Wiley & Sons; 2020.
22. Harikaran GK. Machine Learning Approaches for Predicting Soil Properties of Vemagal Hobli, Kolar District, Karnataka [PhD thesis]. University of Agricultural Sciences, GKVK, Bangalore; 2022.
23. AbdelRahman MAE, Metwaly MM, Shalaby A. Quantitative assessment of soil saline degradation using remote sensing indices in Siwa Oasis. Remote Sensing Applications: Society and Environment. 2019; 13: 53-60. doi: 10.1016/j.rsase.2018.10.004
24. Schoeneberger P, Wysocki DA. Geomorphic Description System, Version 5.0. Natural Resources Conservation Service, National Soil Survey Center, Lincoln, NE, USA; 2017.